American Journal of Mechanical and Industrial Engineering
2016; 1(3): 74-84
http://www.sciencepublishinggroup.com/j/ajmie
doi: 10.11648/j.ajmie.20160103.17

Design Optimization of Pico-satellite Frame for Computational Analysis and Simulation

Anselm Chukwuemeka Okolie[1, *], Spencer O. Onuh[1], Yusuf T. Olatunbosun[1], Matthew S. Abolarin[2]

[1]Department of Mechanical Engineering and Manufacturing, Centre for Satellite Technology Development, Abuja, Nigeria

[2]Department of Mechanical Engineering, Federal University of Technology, Minna, Nigeria

Email address:

okolie.anselm@cstd.nasrda.gov.ng (A. C. Okolie), onuh.spencer@cstd.nasrda.gov.ng (S. O. Onuh), mustbosun@yahoo.com (Y. T. Olatunbosun), abolarinmatthew@yahoo.com (M. S. Abolarin)

[*]Corresponding author

To cite this article:

Anselm Chukwuemeka Okolie, Spencer O. Onuh, Yusuf T. Olatunbosun, Matthew S. Abolarin. Design Optimization of Pico-satellite Frame for Computational Analysis and Simulation. *American Journal of Mechanical and Industrial Engineering.* Vol. 1, No. 3, 2016, pp. 74-84. doi: 10.11648/j.ajmie.20160103.17

Received: September 20, 2016; **Accepted**: October 8, 2016; **Published**: October 31, 2016

Abstract: In this research work, a structural optimization methodology is applied to generate a Frame model that meets CubeSat Design Standards. The frame is further subjected to software simulation that encapsulates worst case launch scenarios. The validity of the frame design has been demonstrated by quasi-static and modal analyses, with the results being verified analytically using direct stiffness approach. All subsystems in this study were modelled as remote masses at their Centre of Gravity (C.G) positions, considering their Moments of Inertia (M.I). The mass location analysis was done for a presumed internal configuration with the subsystems arranged such that the Centre of Gravity (C.G) and Moment of Inertia (M.I) values satisfy the launch vehicle constraints. The mass of the proposed structure has been reviewed to meet design mass requirements of a picosatellite structure as a subsystem with a mass less than 20 per cent of overall design mass of 1.33kg. The frame is modelled to bear the on-board electronics without transferring significant load to these delicate electronics that represent different subsystems. The failure analysis of the final structure design indicates very infinitesimal resultant displacement of 1.573×10^{-2}mm which is far less than a millimetre and a Factor of safety of 2.06. The minimum natural frequency for the first mode of free vibration of the final design structure obtained to be 199.32 Hz indicating very high structural stiffness. The worst-case harmonic and random vibration analyses have been performed on the frame-PCBs assembly. The maximum structural responses- displacement and stress- at critical points on the Printed Circuit Boards (PCBs) yielded 3.733×10^{-4}mm and 98666.7N/m^2 respectively for harmonic excitation. and 1.715×10^{-1}mm and 33090298N/m^2 respectively for random vibration. The peak stress values compared to material yield stress indicate that the subsystems would remain safe under severe launch loading conditions.

Keywords: Vibration, Simulation, Picosatellite Structure, Optimization, Analysis

1. Introduction

In recent times, the high cost of building and launching macro satellites is alarming. As a result, developing countries could hardly afford venturing into space research and programs. Since the cost of building and launching a satellite is a function of its size and weight, there is an urgent need for topology optimization of satellite structures and other subsystems to minimize weight within the specified envelop and to withstand specified loading conditions. International Space Research community are currently putting more efforts to further miniaturize satellites.

Today there are picosatellites, these are satellites of mass between 0.1kg and 1kg, of which their configuration could occur in cubical, hexagonal or cylindrical as the case may be depending on its application and internal space requirement [1].

In this study, a picosatellite of external cubical configuration is considered to meet CubeSat design standards which include that it must occupy a specified envelop of 10 cubic centimeters yet not to exceed 1.33kg of mass; these fundamental features are the physical constraints and

restrictions that points to the technical challenges in CubeSat structural designs inspiring researches in many sectors of CubeSat development [2]. The CubeSat program is a global research work which involve various universities, high schools and private corporations. The program was initiated mutually by California Polytechnic State University and Stanford University in 2003 and has been sustained by others with more universities and industries all over the world gaining more and more grounds in many sectors of CubeSat research [3].

At the onset, the CubeSat concept served as an educational tool. The development of this concept by the pioneers thus became a learning process, to afford students an opportunity to explore satellite technology and engineering [4]. The cost of miniaturization is in the complexity of the satellite structural design and so the structure of the satellite must be simulated and analyzed in details to examine its structural integrity, while it is being optimized to minimize material as well as cost.

Many picosatellite structural concepts have been suggested for specific design requirements by various institutions worldwide. In [5], an overall configuration process of a cubesat model was presented. The static analysis performed on the model was done with ANSYS. Aluminum 6061-T6 was considered for both the primary and secondary structure with a fixed-free boundary constraint. The launch requirements for the work was based on Arian Structure for Auxiliary Payloads (ASAP) such that the static acceleration load of 10g was applied along the three principal axes. However, the maximum stress of 40.055 Mpa occurred along x-axes lateral loading. This value implies that the strength requirement was met when compared to material yield strength. In the same vein, the minimum natural frequency of the structure generated is 180.68Hz which is higher than stipulated excitation frequency of launch vehicle. Thus, stiffness requirement was met.

Similarly, [6] detailed the modal, harmonic and random vibration analysis of a structurally optimized nano-satellite using ANSYS. The launch load data were derived from Polar Synchronus Launch Vehicle (PSLV) provided by Indian Space Research Organization. The static inertial loads imposed on the structure to evaluate its strength characteristics are as follows: ± 11g along z-axis, ± 6g along y-axis and ± 6g along x-axis with a safety factor of 1.5 incorporated on each load case. In this work static analysis was not reflected; however, the modal analysis result shows that the launch vehicle excitation frequency benchmark of 100Hz was exceeded as the first minimum frequency of 178.98Hz was generated. The maximum normal stress and deformation of 0.123Pa and 1.95 x 10^{-10}mm respectively occurred at approximately 183Hz under 2.75g lateral harmonic loading between frequency band of 20 and 200 Hz considering 10 calculation sub steps. Similarly, the random vibration result indicates maximum normal stress of 2.6MPa and 5.90 x 10^{-3}mm deformation. It was inferred from these values that the proposed design will not yield or deform throughout launch.

The frame is the primary structure and main load-bearing component of the structure subsystem. For an efficient frame design, the loads that it must bear through launch, must be evaluated under realistic conditions during simulation, and must satisfy stiffness and strength requirements based on the desired launch vehicle. In this work, harsh launch loading scenarios were simulated to ensure the frame could withstand high g-forces and dynamic loads, without significant deformation on the printed circuit boards (PCBs) with sensors and actuators on-board during launch. The aim of this study, is to demonstrate the preliminary design optimization of a pico-satellite modular frame, of cubical configuration, to meet the launch vehicle requirements while maintaining pico-size and bearing internal loads. The computer aided design (CAD) model of the frame was generated and converted to analysis suitable model by meshing to obtain the finite element results. The loads and physical constraints were imposed prior to analysis. The stresses, displacements and strains at critical points of the frame design were evaluated, analyzed and compared at various load conditions.

2. The Pico-satellite Design Concept

This structural concept was designed to ensure ease of assemble, access to internal components and rigidity. There are two single side piece brackets that make up the modular frame and they are separated by four cross bars referred to as the shear bars. The identical side piece bracket comprises of two bars held in position by another set of cross bars referred to as support bars (Figure 1). This support bar has direct contact with the tie bars, which directly bears the bending moment induced by the PCBs and the mounted components, and also transfers the internal loads to the frame (Figure 2).

The single side piece frames in this design minimize the amount of fasteners thereby increase structural strength against vibration. The configuration comprises of four stack-up PCBs screwed along tie bars to the support bars, which in turn transfers load to the rest of the frame structure.

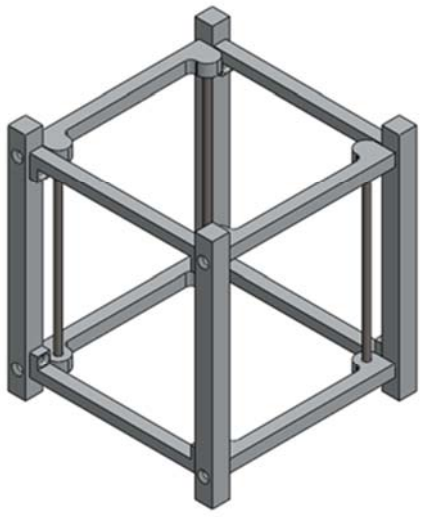

Figure 1. *CAD model excluding PCBs.*

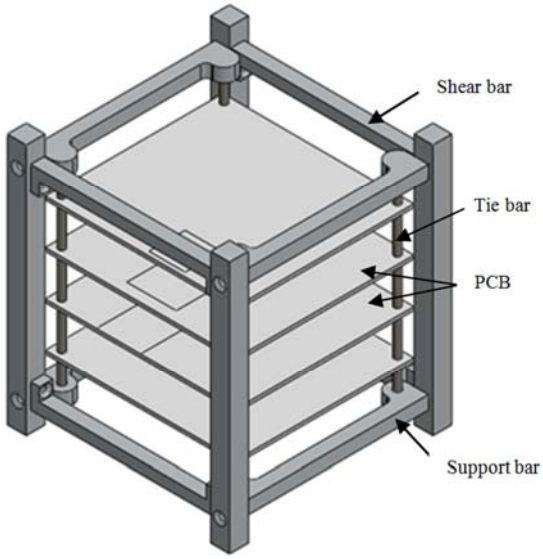

Figure 2. *CAD model with PCBs.*

3. Material Selection

In this study, our material of choice for the frame is Aluminum 6061-T6 due to the following characteristics [7]:

a. Its strength-to-weight ratio is very high making it ideal for attaining a light-weight structure.
b. Excellent structural strength and toughness, indicating high stiffness and workability.
c. It has good finishing characteristics and responds well to anodizing.
d. It is readily available and has excellent machinability due to its chip characteristics.
e. Excellent joining characteristics and thermal expansion coefficient similar to that of the Poly-Picosatellite Orbital Deployer (P-POD) material, Al 7075-T73.

3.1. Design Constraints

For the scope of this work, the exterior design specifications and constraints are defined within Cubesat standards. The single unit structure must adapt to the standard picosatellite deployer system, which is the P-POD pre-designed for CubeSats. As a result, the lateral section of the satellite must have its dimension span 100.0 ± 0.1mm in width, while its longitudinal section must span 113.5 ± 0.1mm and the weight is not to exceed 1.33kg. The structure alone should not take more than 30% of the total satellite weight. Similarly, the centre of mass of the satellite must fall within 2cm of its geometric centre [8].

3.2. Launch Load Levels

The design loads calculated for this work were derived based on the Dnepr launch vehicle specifications. Considering the inertial and dynamic loads imposed on the satellite during launch due to high levels of acceleration, vibration and shocks experienced by the launch vehicle, the designed satellite frame must be able to withstand and strictly comply with the specified loading levels without permanent deformation, as shown in Table 1 to Table 4.

Table 1. *Quasi-static loading level [9].*

	Load factors	Max. load factor	Factor of Safety	Inertial load
X-axis	0.5 ± 0.5g	1.0g	1.5g	1.5g
Y-axis	0.5 ± 0.5g	1.0g	1.5g	1.5g
Z-axis	7.8 ± 0.5g	8.3g	1.5g	12.45g

Table 2. *Amplitude of Harmonic Oscillations at SC/LV Interface Launch Axis (Z) [9].*

Frequency sub-band, Hz	Amplitude, g	Duration
5-10	0.5	10
10-15	0.6	30
15-20	0.5	60

Table 3. *Amplitude of Harmonic Oscillations at SC/LV Interface Lateral Axis (X, Y) [9].*

Frequency sub-band, Hz	Amplitude, g	Duration
2-5	0.2-0.5	100
5-10	0.5	100
10-15	0.5-1.0	100

Table 4. *PSD values in use for Random loading level [9].*

Frequency band, Hz	Qualification PSD (g^2/Hz)	Acceptance PSD (g^2/Hz)
20-40	0.007	0.007
40-80	0.007	0.007
80-160	0.007-0.022	0.007
160-320	0.022-0.035	0.007-0.009
320-640	0.035	0.009
640-1280	0.035-0.017	0.009-0.0045
1280-2000	0.017-0.005	0.0045
Root mean square value, σ, g	6.5	3.6
Duration, sec	35	831

3.3. Stiffness Requirement

The frequency constraints for this work is to be placed on a higher stiffness requirement benchmark than was stipulated in [9]. The following values were therefore used as base excitation frequency of the launch vehicle to ensure very high structural stiffness:

First natural frequency along longitudinal axis: >100Hz
First natural frequency in the lateral axis:> 50Hz

4. Simulation and Analysis of the Structure

The modular frame is initially geometrically idealized and modelled excluding joints and connectors using SolidWorks. The simplified model is optimized to obtain appropriate sizing of the design sections that could bear internal and external launch loads while maintaining minimum weight. The strength and stiffness requirements are met by the frame prior to integrating the internal printed circuit boards (PCBs). The structure is further subjected to linear dynamic analysis with internal components incorporated to further ensure structural integrity.

4.1. Design Study to Generate Optimal Frame

The initial Frame model shown in the Figure 3 weighed 74 grams. The other design variables considered for the optimization are detailed in Table 5.

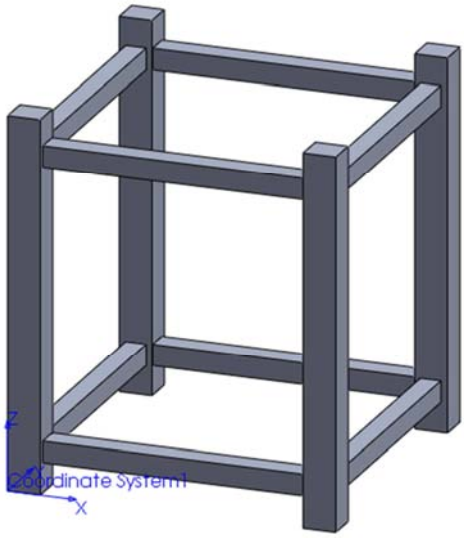

Figure 3. *Initial Frame Design Model.*

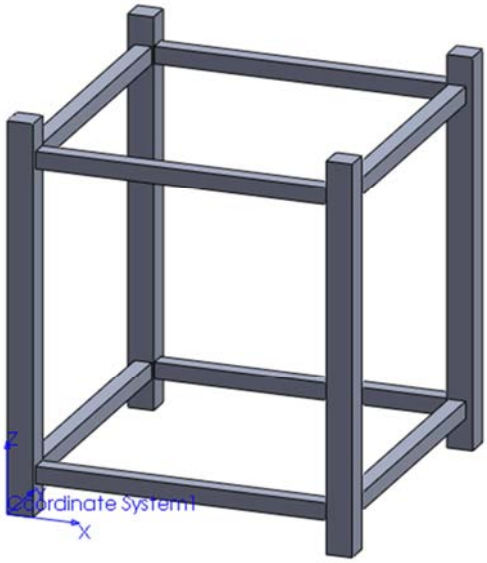

Figure 4. *Optimized Frame Model after running Design Study.*

The resultant optimal frame generated after running through 41 iterations of design study is shown in Figure 4. The minimal mass of 42.54 grams was achieved. The optimal design variables that satisfied all constraints and met the desired objective are shown in Table 6.

Table 5. *Design variables and constraints.*

Design variables: initial (mm)	Range (mm)	Constraints
Rail section width D_1: 10	$7.5 \leq D_1 \leq 10.0$	Effective stress < 275MP
Support bar section L, D_{2Y}: 6.5	$5.0 \leq D_{2Y} \leq 8.0$	Resultant displacement < 1mm
Support bar section W, D_{2X}: 6.25	$5.0 \leq D_{2X} \leq 7.5$	Displacement at free end, Z<0.005mm
Shear bar section L, D_{3Y}: 6.5	$5.0 \leq D_{3Y} \leq 8.0$	First axial natural frequency > 100Hz
Shear bar section W, D_{3X}: 7.5	$5.0 \leq D_{3X} \leq 7.5$	

Table 6. *Optimal design values generated.*

Design variables	Optimal values (mm)
Rail section width, D_1	7.5
Support bar section L, D_{2Y}	5.0
Support bar section W, D_{2X}	5.0
Shear bar section L, D_{3Y}	5.0
Shear bar section W, D_{3X}	5.0

4.2. Analysis Set up

The frame design generated earlier becomes the basis to set up an analysis model for detailed verification of the structural integrity of the frame. The optimal frame model is first split into the different component modules and then assembled as shown in Figure 1.

The PCBs are incorporated on the frame and the internal components are mounted on it such that moment of inertia and center of gravity requirements are satisfied, refer to Table 7. These internal components are simplified as blocks of mass and treated as remote loads positioned by means of a spreadsheet mass location analysis.

According to [10], the external loads on the structure are calculated as follows:

In the longitudinal direction, the Design Limit Load on the frame is:

$$F_{limit,z} = F_{sats,TENSION/COMP.} + F_{springs}$$

$$= (\text{No. of Sats x Design Mass x } N_z) + F_{springs} \quad (1)$$

In the lateral direction, the Design Limit Loads on the frame becomes:

$$F_{limit.X,Y} = F_{sats,BENDING} + F_{springs}$$

$$= (\text{No. of Sats x Design Mass x } N_{x,y}) \quad (2)$$

$$F_{resultant} = \sqrt{\left(F^2_{limit,z} + F^2_{limit.x,y}\right)} \quad (3)$$

No. of Sats refers to the two satellites which the design structure must carry in a vertically oriented P-POD arrangement during launch. Design mass is based on CDS rev 12 of 1.33kg for 1-unit Cubesat.

N_z = Inertia load factor along longitudinal axis (Z)

$N_{x,y} = N_x = N_y$ = Inertial load factor in lateral axes of X and Y respectively.

These are the inertia load factors calculated after incorporating a safety factor of 1.5, refer to Table 1, which is a little higher than the one considered in [11] for spacecraft structures design load.

4.2.1. Connectors

Bolted screw joint connectors were considered for the analysis set up. The material of the screw is space qualified stainless steel (SS304) M3 × 0.45 mm screws, and the calculated bolt pretension was 563.45 N, as recommended by the guidelines suggested in [12].

4.2.2. Boundary Conditions

The model is expressed as vertically positioned beam with fixed-free end condition based on its launch configuration. The design structure bears the external loads which include the weight of the two standard CubeSats of 1.33kg each and the high g-loads due to launch vehicle, Figure 5.

Table 7. *Mass-location Analysis (Experimental).*

Component	Mass M(g)	Position (r)			Mass x Position		
		x(mm)	y(mm)	z(mm)	(gmm)	(gmm)	(gmm)
Payload	120	50	50	50	6000	6000	12840
GPS	21.5	60	20	20	1290	430	1870.5
Micro-controller	40	50	26	26	2000	1040	2680
Structure	491	50	50	50	24550	24550	27987
Comm	32	50	65	65	1600	2080	1504
Attitude	32	40	20	20	1280	640	1504
EPS	162	50	65	65	8100	10530	4374
	898.5				44820	45270	52759.5
CG		49.883	50.384	58.72			
GC		50	50	57			
ABS (GC-CG)		0.117	0.384	1.72			

$$CG = \frac{\sum M \, x \, r}{\sum M} \tag{4}$$

The static analysis model shown in Figure 6 depicts the remote loads applied at the centre of gravity location of the block masses. The frequency model has no load application as indicated in Figure 7, thus, the body weight of the frame is all that is considered for the modal analysis.

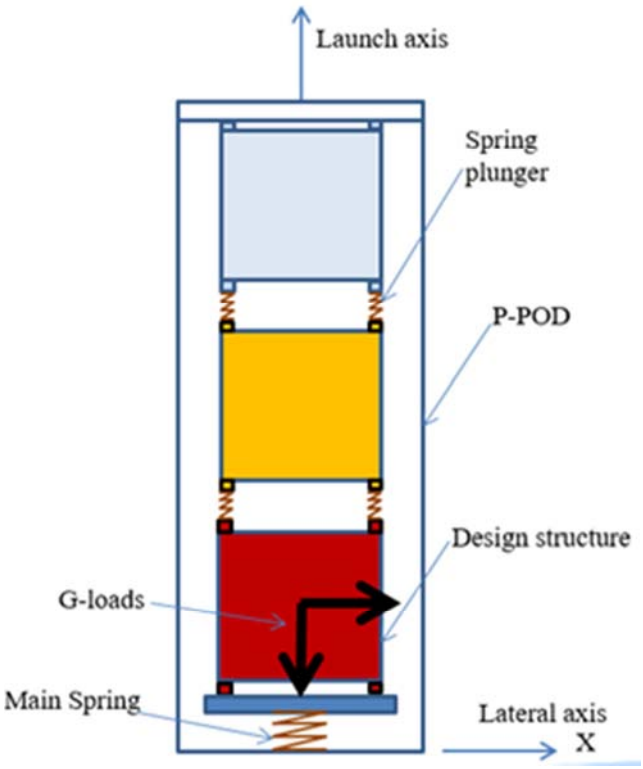

Figure 5. *Schematic representation of the worst case launch configuration.*

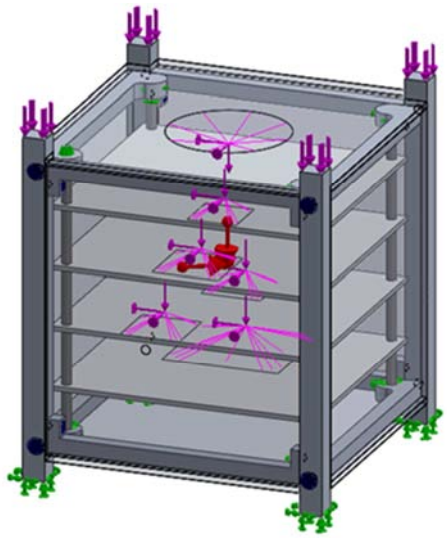

Figure 6. *Static Analysis Model.*

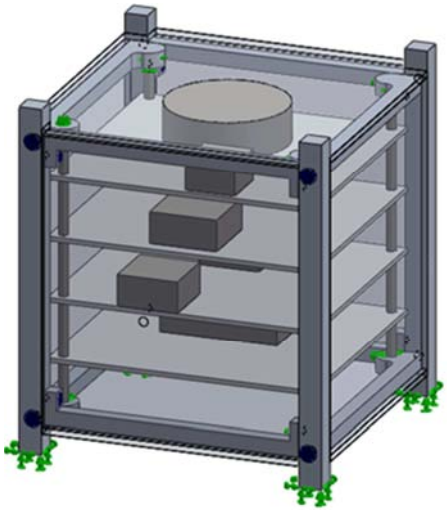

Figure 7. *Frequency Analysis Model.*

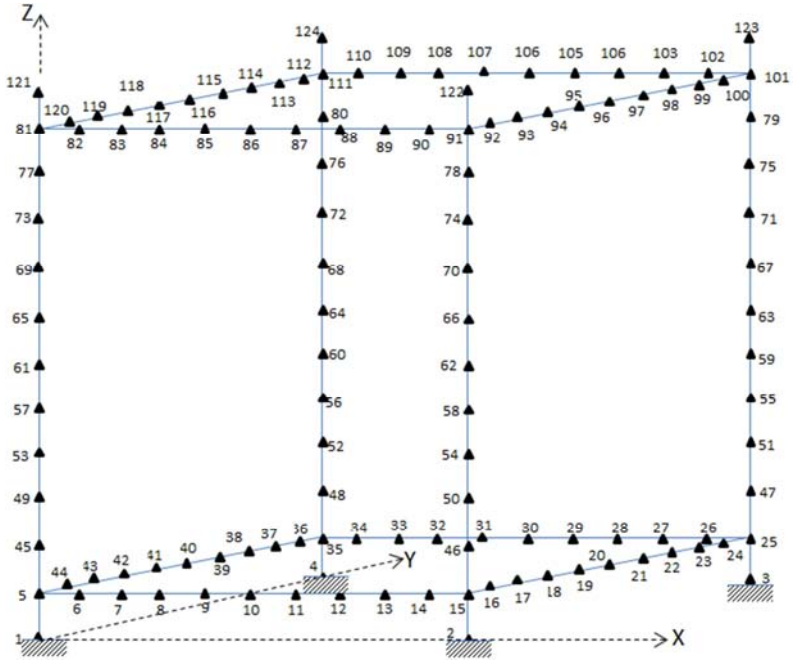

Figure 8. *Discretized Domain for MATLAB computations.*

As shown in the Figure 8, the nodes 1, 2, 3 and 4 are grounded; and therefore have zero translational and rotational displacements. The boundary conditions are thus:

$$U_{1x} = U_{1y} = U_{1z} = Ø_{1x} = Ø_{1y} = Ø_{1z} = 0$$

$$U_{2x} = U_{2y} = U_{2z} = Ø_{2x} = Ø_{2y} = Ø_{2z} = 0$$

$$U_{3x} = U_{3y} = U_{3z} = Ø_{3x} = Ø_{3y} = Ø_{3z} = 0 \quad (5)$$

$$U_{4x} = U_{4y} = U_{4z} = Ø_{4x} = Ø_{4y} = Ø_{4z} = 0$$

At nodal points of load on the rail, that is, nodes 121, 122, 123 and 124, the resultant load imposed due to the weight of the two aforementioned CubeSats on-board is calculated from equation (3) such that the applied load at the contact surface of each rail cross-section is approximately equal to 178.1756 N.

The high g-loads of Table 1 are equally applied on the structure's centre of gravity.

5. Results and Discussion

5.1. Static Analysis

The Picosatellite frame was first considered alone under high g-loads and external forces. The maximum von mises stress of 134.34 x 10^6N/m^2 occurred at the countersink screw hole shown in Figure 9. This value is up to 48.85% of yield stress giving a factor of safety of 2.05. Similarly, the maximum resultant displacement of 6.028 x 10^{-3}mm, which is far less than 1mm, occurred at the point of loading as shown in Figure 10. Thus the total deformation on the frame due to static loading is very negligible

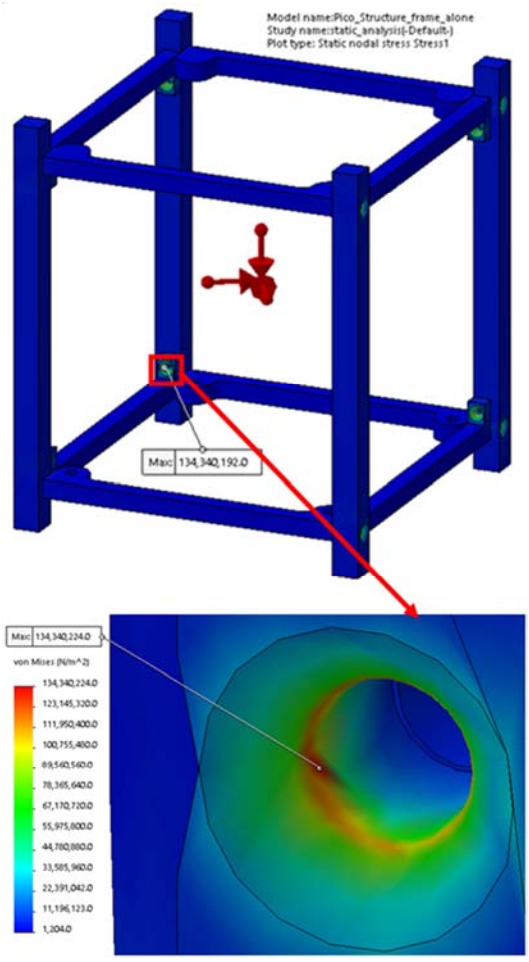

Figure 9. *Maximum Static Nodal stress on Frame.*

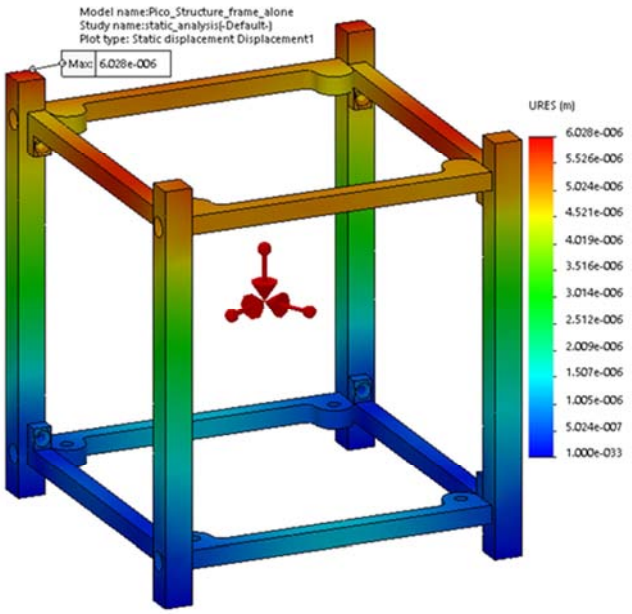

Figure 10. *Maximum resultant displacement on Frame.*

The Table 8 shows structural responses normal to launch/longitudinal axis (Z) at critical point of loading comparing solidworks generated values with MatLab values.

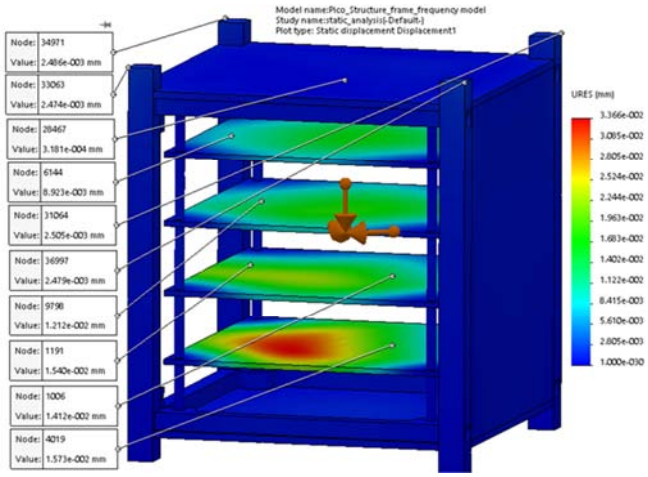

Figure 11. *Resultant displacement at critical nodal locations.*

Table 8. *Maximum normal displacement, stress and strain at critical point of loading.*

	FEM	Max. normal displacement u_z (mm)	Max. normal stress σ_z (N/mm^2)	Max. normal strain ε_z
1.	Matlab	-5.218 x 10^{-3}	-3.1676	-4.5973 x 10^{-5}
2.	SolidWorks	-4.686 x 10^{-3}	-3.1417	-4.485 x 10^{-5}
3.	%Error with respect to 1.	10.2%	0.8%	2.4%

The major structural components- the PCBs and side panels- are incorporated into the analysis model to examine overall structural response under steady-state loading. The Figure 11 indicates that the maximum resultant displacement of 1.573 x 10^{-2}mm (less than 1mm) occurred on the EPS board at Node 4019. The factor of safety of the design structure generated, which is approximately 2.06 guarantees that the frame will not fail during launch, refer to Figure 12.

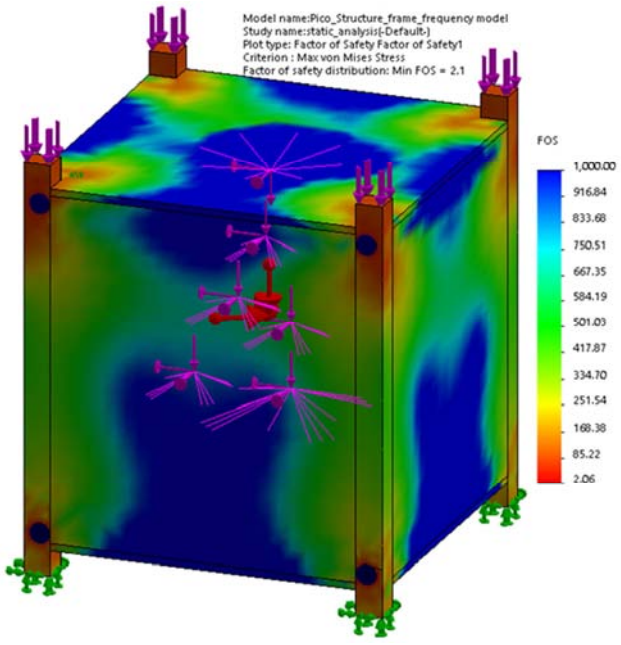

Figure 12. *Factor of Safety distribution on the structure.*

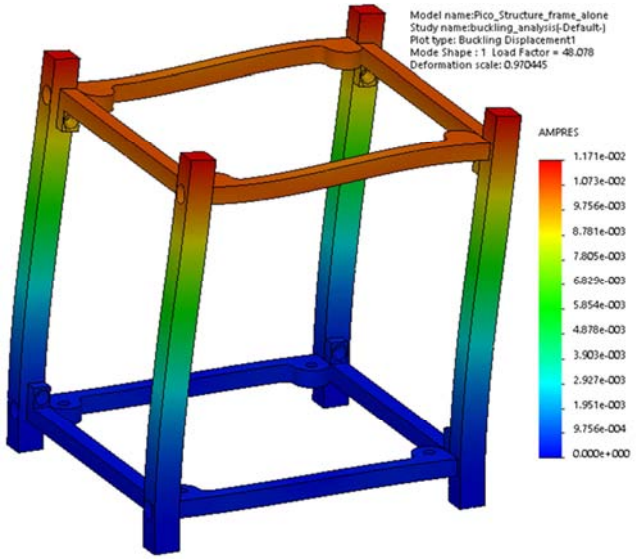

Figure 13. *First mode shape of the Frame buckling analysis.*

The result of buckling analysis on the frame gives a minimum buckling load factor of 48.078 as indicated in Figure 13. This rules out the possibility of the frame ever buckling during launch.

5.2. Modal Analysis

The fundamental frequency of the structure representing the frequency of vibration of the first modal shape is generated as shown in Figure 14 to be approximately 199.32Hz. The maximum resultant amplitude at resonance

occurred at the EPS nodal location. A total of 30 modes of vibration were generated for the frequency response analysis.

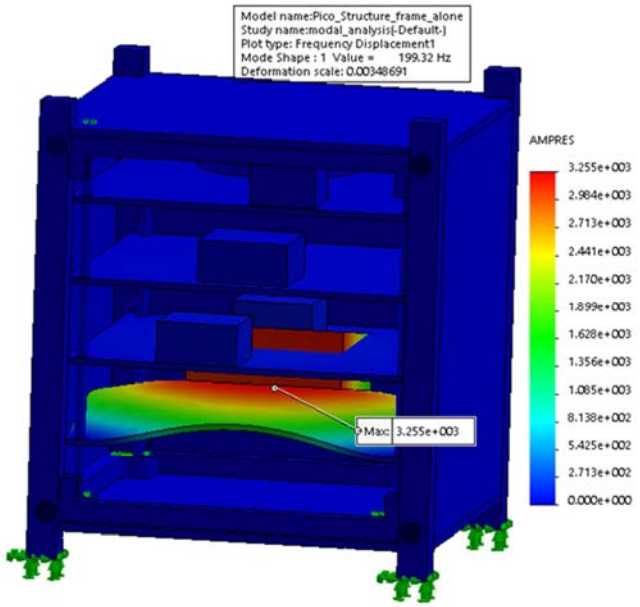

Figure 14. *First mode shape of the structure modal analysis.*

However, this first mode natural frequency of the structure is greater than 100 Hz based on global stiffness requirements. This implies that the design structure is far decoupled from the base excitation frequency of the launch vehicle and would maintain high dynamic stability during launch.

Table 9. *The first ten modal frequencies of the design structure.*

Mode No	Frequency (Hz)
1	199.32
2	238.19
3	268.19
4	318.62
5	364.75
6	390.6
7	421.36
8	433.52
9	490
10	529.61

5.3. Harmonic Analysis

The loads applied for this analysis are derived from Tables 2 and 3 for longitudinal (launch axis) and lateral loading respectively. The results generated were for nodal locations of critical structural response. The frequency response graphs for stress and displacement normal to the longitudinal axis are obtained within frequency range of 5 and 200Hz. All 30 modes of vibration were used for analysis.

Table 10. *Results of harmonic analysis.*

Loading	Maximum normal stress along Z-axis (N/mm^2)	% of yield stress	Maximum normal displacement along Z-axis (mm)	Frequency, Hz (Average value)
Lateral X	678157	0.25	$4.796x10^{-5}$	170.43
Lateral Y	584000	0.21	$7.489x10^{-5}$	170.43
Longitudinal Z	98666.7	0.036	$3.733x10^{-4}$	193.65

In the course of longitudinal harmonic loading, the peak values of stress and displacement occurred at average frequency of 193.65Hz as shown in Table 10, which is near, but does not coincide with the first mode frequency of the structure. This shows consistency with the modal analysis result obtained and assures that no dynamic coupling will occur during this launch loading scenario. Figure 15 and Figure 16, respectively, shows the peak normal stress and normal displacement against frequency under longitudinal harmonic loading. The peak normal stress is evaluated as 98666.7N/m^2 at 193.80Hz as shown in Figure 15, while the peak normal displacement is evaluated as 3.7333 x 10^{-4}mm at 193.5 Hz, refer to Figure 16. Similarly, for lateral harmonic loading, the Figure 17 shows a peak normal stress of 678157N/m^2 occurring at 170.236Hz while the peak normal displacement of 7.48889 x 10^{-5}mm generated in Figure 18 occurred at 170.389Hz. The percentage of the resulting normal stress, in both load cases, relative to the material yield stress is very insignificant, meaning no yielding would occur due to applied harmonic loading. Normal displacement responses to both longitudinal and lateral harmonic loading are far less than one millimeter, and thus, cannot cause any permanent deformation on the structure.

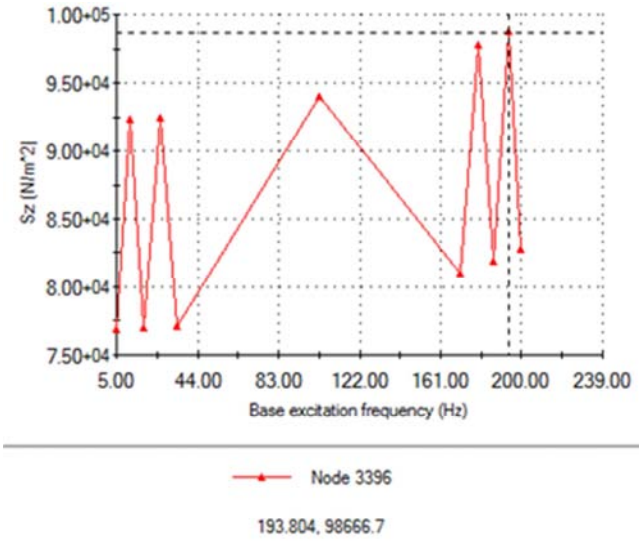

Figure 15. *Normal stress against frequency (Longitudinal).*

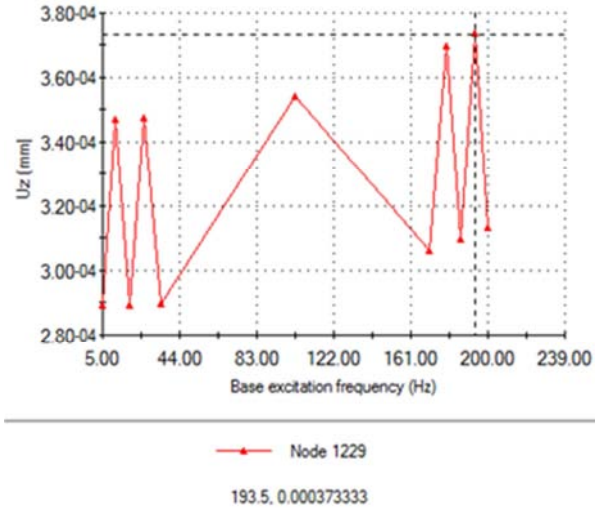

Figure 16. *Normal displacement against frequency (Longitudinal).*

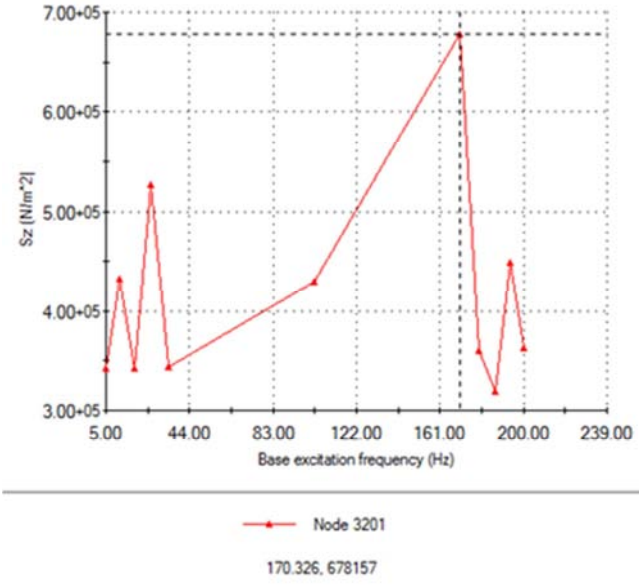

Figure 17. *Normal stress against frequency (Lateral).*

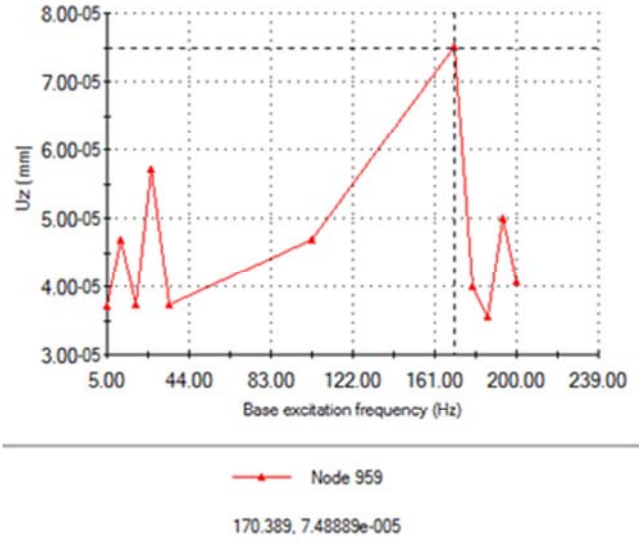

Figure 18. *Normal displacement against frequency (Lateral).*

5.4. Random Vibration Analysis

The loads for this analysis are derived from Table 4. The results generated were for nodal locations of critical structural responses of stress, displacement and acceleration expressed in root mean square (RMS). The power spectral density (PSD) response graphs at peak nodal locations of the structure for stress, displacement and acceleration were obtained within frequency range of 5 to 200Hz. All 30 modes of vibration were used for analysis.

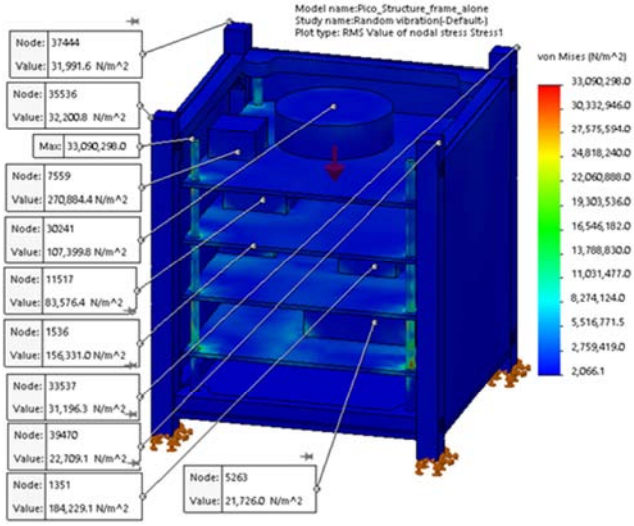

Figure 19. *RMS value of von mises stress at critical nodal points.*

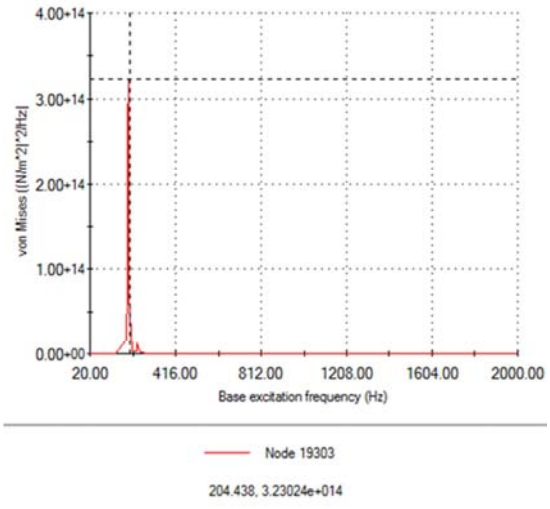

Figure 20. *Excitation frequency at which peak von mises stress occurred.*

The maximum RMS von mises value generated is approximately 33.09MPa, which is far less than material yield stress, and occurred at the tie bar interface with the support bar, Figure 19. The excitation frequency on which maximum stress response occurred is derived from the PSD stress response graph of Figure 20. The value is 204.44Hz and the node 19303. Also, the maximum RMS value of the resultant displacement generated is 1.715 x 10^{-1}mm (Figure 21) occurring at a nodal location where the electrical power system EPS PCB is positioned, node 5725. The

excitation frequency at this peak displacement is 195.77Hz as indicated in Figure 22.

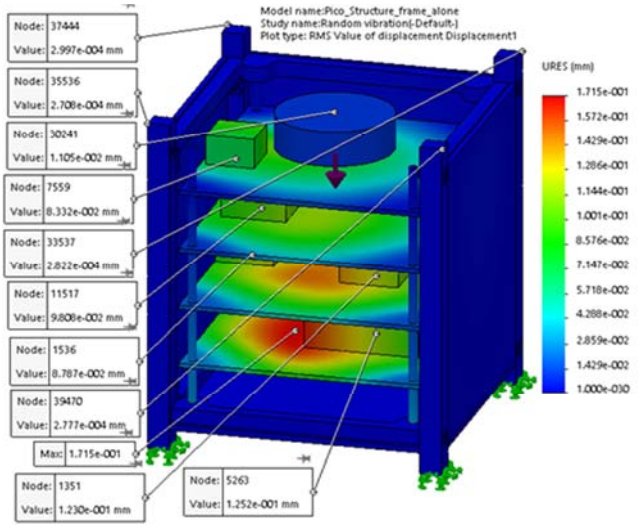

Figure 21. *RMS value of resultant displacement at critical nodal points.*

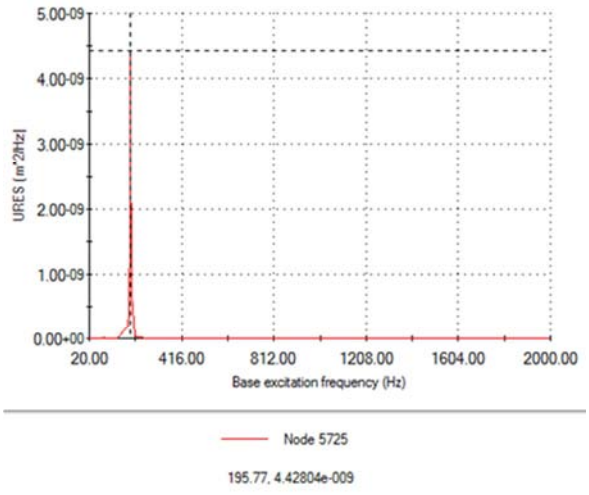

Figure 22. *Excitation frequency at which peak resultant displacement occurred.*

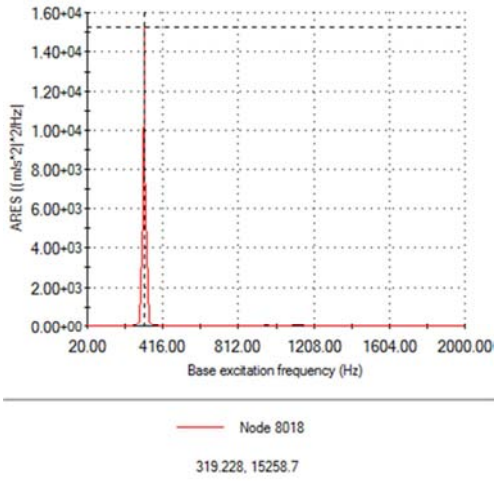

Figure 23. *Excitation frequency at which peak resultant acceleration response occurred.*

The peak acceleration response with respect to the random vibration, however, occurred at the edge of the communications PCB, node 8018 to be precise, with a frequency of 319.228Hz, see Figure 23.

Table 11. *Results of Random vibration analysis.*

	Peak Von Mises Stress (N/m^2)	**Peak Resultant Displacement (mm)**	**Peak acceleration (m/s^2)**
RMS value	33090298	1.715×10^{-1}	4.512×10^{-4}
Frequency of occurrence (Hz)	204.44	195.77	319.23
Node	19303	5725	8018

The structural responses to the random loading as shown in Table 11 indicate that the frame and PCBs will survive all random loading scenarios during launch. This implies that any fragile electronic component onboard the PCB will not experience deformation or failure due to the imposed launch load conditions. The RMS values are not in any way close to failure limits. To further establish structural integrity and safety of onboard components, the excitation frequencies corresponding to these peak responses does not coincide with modal frequencies, which implies no resonance or extreme acceleration responses. Thus, the structure is safe.

6. Conclusion

The study has been able to actualize a launchable picosatellite frame with optimal sectional sizes of rails, support bars and shear bars that can bear high launch loads of worst-case launch configuration in a P-POD. The optimal design analyzed for quasi-static, modal, harmonic and random response based on the loading specifications of Dnepr launch vehicle (LV) proved reliable. The resultant von mises stress on the structure due to quasi-static loading is up to 48.85% of yield stress giving a factor of safety of 2.05. Similarly, the maximum resultant displacement obtained, 6.028×10^{-3}mm is negligible.

The first modal frequency of the design structure, 199.32Hz, is far decoupled from the minimum frequency requirement of Dnepr LV. The linear dynamic analyses are consistent with modal analysis results. For harmonic and random vibration analyses, no incidence of resonance was recorded which implies that the peak stress and displacement responses generated do not occur at excitation frequencies corresponding to the modal frequencies of the structure. These peak responses due to harmonic and random loading are far within considerable safe limits which affirms the safety of any internally mounted component on the PCBs. The analyses results were verified theoretically using direct stiffness approach with MatLab. The validation by assembly and real vibration tests will be established in the subsequent phases of this work.

Acknowledgements

We are grateful to the Mechanical Engineering and Manufacturing Department of the Centre for satellite Technology Development and the Management of National Space Research and Development Agency for their contributions to the success of this work. Also, special appreciation goes to Engr. B. Alkali of Mechanical Engineering Department Federal University of Technology Minna, whose ideas and critics were of immense value.

References

[1] Sarafin, T. P, Larson W. J., Spacecraft Structures and Mechanisms-From Concept to Launch. Microcosm Press and Kluwer Academic Publishers, Torrance, CA, pp. 523-524, 1995

[2] Pierlot, G., OUFTI-1: Flight System Configuration and Structural Analysis, Aerospace and Mechanical Engineering Department, University of Liege, pp. 1-2, June 2009

[3] Cihan, M., A Methodology for the Structural Analysis of CubeSat, Istanbul Technical University, Faculty of Aeronautics and Astronautics, pp. 14-18, Jan. 2008.

[4] Paluszek, M., De Castro, E., Hyland, D., The CubeSat book, Plainsboro, New Jersey, pp. 3, 2010.

[5] Moustafa E., Abdul R. E., Zafar M., Emirates Aviation College CubeSat Project: Tuning of Natural Modes, Static and Dynamic Analyses of the Strength Model, Aeronautical Engineering Department, Emirates Aviation College, Dubai, UAE, pp. 29-32, 2011.

[6] Srikanth R., Nagaraj S. N., Dynamic Analysis and Verification of Structurally Optimized Nano-Satellite Systems, Journal of Aerospace Science and Technology 1, doi: 10.17265/2332-8258/2015.02.005, pp. 78-90, 2015.

[7] http://www.sapagroup.com/en/na/profiles/6061-t6-aluminium-properties/. Retrieved in June, 2014

[8] Munakata, R., CubeSat Design Specification, Revision 12, Calpoly SLO, pp. 7-9, 2009.

[9] Stanislav, I. U., Dnepr Space Launch System (SLS) User Guide, completely revised issue 2, Moscow, pp. 54-56, Nov., 2001.

[10] Wong, S., Whipple, L., Dolengewicz, J., The Next Generation CubeSat: A Modular and Adaptable CubeSat Frame Design, California Polytechnic State University, San Luis Obispo, pp. 40-41, 2010.

[11] Wijker, J., Spacecraft Structures, Springer-Verlag Berlin Heidelberg, 15-16, 107-108, 2008.

[12] Budynas, R. G., Nisbett, J. K., Shigley's Mechanical Engineering Design-9th Ed. McGraw-Hill Companies, Inc., 1221 Avenue of Americas, New York, NY 10020, pp. 437-438, 2011.